Rule Based Electricity Price Responsive Control for HVAC System Using Thermal Energy Storage

Andreas J. Poulsen, Christian V. Østerballe, Jan Peter M. Christiansen,
Jonas L. Jørgensen & Nicolai D. Dannesbo
Control and Automation Section, Department of Electronic Systems, Aalborg University, Aalborg, Denmark
Email: [ajpo18, cvas18, jpmc18, jlja18, ndanne18] @student.aau.dk

***Abstract*—Consumers are interested in reducing their total electricity cost. Due to fluctuations in electricity cost, this may be achieved by introducing flexibility in consumption periods which, in heating-, ventilation- and air-conditioning (HVAC) systems, is achievable by utilising a thermal energy storage (TES). This paper details the design of a control structure, capable of shifting loads based on forecast electricity prices, while keeping the room temperature stable. The system is split into two operation modes, charging and discharging, which are modelled using state space equations, fitted to experimental data, and simulated in Simulink. The control structure consists of a cascading PI controller, for which the inner control loop depends on the operation mode. A Rule Based Controller (RBC) is designed, which takes into account the forecast electricity price to determine the operation mode. Simulations show that the RBC is capable of reducing the total electricity cost by up to 6.6 % while keeping the room temperature within 1 °C of its reference.**

***Index Terms*—HVAC, TES, RBC, Electricity Cost Reduction, State Space Modelling**

I. Introduction

ENERGY production and consumption vary throughout the day causing fluctuations in the electricity price [1]. On the consumer side, there is an interest in reducing total electricity costs, which may be achieved by a consumption shift, increasing consumption when it is cheap and reducing consumption when it is not.

One method of introducing flexibility in heating-, ventilation- and air-conditioning (HVAC) systems, is by utilizing a water tank and the thermal capacity of the building itself [2]. By adjusting the output of a heat pump to utilize the thermal storage prior to a peak period, less heating is needed in this period, reducing the peak consumption. The peak period is a constant 3-hour window each day. Another method utilizes the current electricity price by forcing the heating on when the price falls below some threshold and forcing it off when it goes above some threshold, storing excess heat in a water heat storage [3]. These thresholds are determined by modeling the price as a normal distribution and using its mean and standard deviations. If a forecast of the electricity is available, the controller may use the ratio between the current and the forecast peak price as a control variable instead [3].

The hypothesis is thus: It is possible to construct and implement a rule-based controller capable of reducing the total electricity costs of operating an HVAC system by shifting loads according to forecast electricity price, while staying within a comfortable temperature range. The goal of this paper is to design and implement such a controller on the HVAC test bed at AAU Campus Aalborg. The focal point of this paper is to model the system and implement local controllers, such that a price responsive controller is implementable. These models and controllers rely on previous work on the test bed, such as a controller for the heat pump and existing communication infrastructure.

In this paper a test bed description, an overview of the control configuration and a data-acquisition & remote control interface is given in Sec. II. Models for the system are constructed and presented in Sec. III. Based on these models, controllers are designed, which are presented in Sec. IV. This includes the price responsive RBC. Sec. V presents simulation results of the models and controllers conducted in Simulink.

II. System Description

A. Test Bed Description

The HVAC test bed consists of three systems as seen in Fig. 1: A heat pump, a thermal energy storage (TES), and a ventilation system. Heat from the heat pump is exchanged with the TES, i.e. a water tank capable of storing excess energy. The heated water flows through a heating coil, heating air in the ventilation system, which is transferred to the target room via fans. The TES system includes two valves, one capable of redirecting hot water to the water tank and one capable of bypassing the water tank when using stored energy to heat the air. In the ventilation system, it is possible to use fresh air from outside or re-circulate and re-use the air from the target room. The energy supplied by the heat pump can be adjusted within a range and the heat pump may be turned on or off with some minimum switching time.

B. System Overview

The overall strategy is to use electricity when it is cheapest, but still control the temperature in the target room within some range. By storing energy when electricity is cheap and using it when electricity is expensive, the total electricity cost may be reduced.

Fig. 2 shows a schematic of the control hierarchy which includes a room temperature controller. This controller uses the target room temperature as feedback together with the target room reference temperature, to determine the needed output temperature of the heated air, $T_{a,ref}$. This air temperature is used as a reference for the inner controllers. The system has

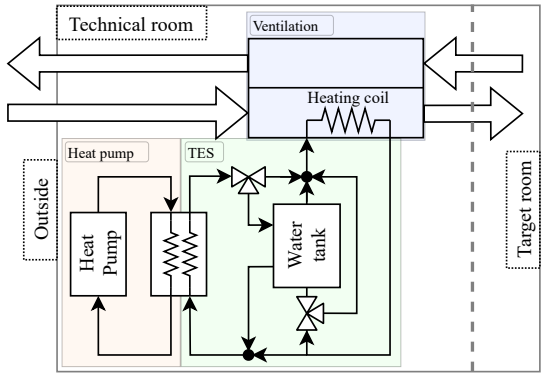

Fig. 1. A functional overview of the HVAC test bed.

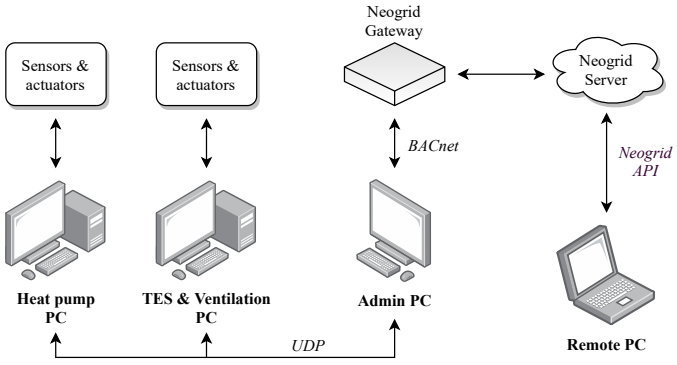

Fig. 3. Schematic of the communication setup for data acquisition and remote control of the HVAC test bed.

two operation modes. These operation modes are defined to utilize the energy storing capability of the water tank. In charging mode, the heat pump is on and some of the heated water flows through the heating coil while some of it flows through the water tank. The ratio between these two flows is controlled by a valve. The charging mode controller is responsible for delivering the correct air temperature to the target room as well as controlling the excess power generation such that the water tank can reach a targeted temperature. In discharging mode, the heat pump is off and only energy stored in the water tank is utilized to achieve the correct air temperature to the target room. The temperature of the water in the heating coil is controlled by mixing the water from the tank with the return water from the heating coil, by adjusting the opening of a valve. Finally, the price responsive RBC determines the operation mode and tank set-point by considering the current electricity price compared to the forecast price and the current state of the system.

C. Communication Interface

To facilitate the use of the current and forecast electricity price, a communication interface is designed, such that the RBC is capable of accessing the internet, further enabling the possibility to run the controller remotely. The communication interface is built on top of existing communication infrastructure on the test bed. Fig. 3 shows an overview of the remote access system. The remote access is made possible by a server & gateway supplied by the company Neogrid. Each sensor is sampled every 10 seconds and this data can be pulled by a request protocol on a remote PC. This remote PC may also adjust actuator values affecting the actuators on the test bed, thereby allowing full remote control of the system.

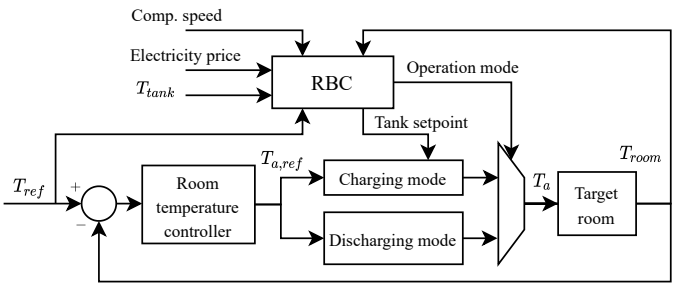

Fig. 2. Diagram of the system and selected control configuration.

III. Modeling

The two operating modes share common elements for which models are constructed and presented in this section. The specifics of each mode are first detailed and elements unique to each mode are then modeled. The diagram of the two modes are seen in Fig. 4 and Fig. 5 respectively. In the figures, mass flows are represented by the variable m and temperatures by T. Variables sub-scripted with a correspond to air and w to water.

A. Modeling of the Heating Coil

The heating coil is split into N partitions for both the water and air side to describe the temperature change through it. Each partition is coupled to the previous through the flow of fluid m and to the corresponding partition on the other fluid's side by the conductance G_{hc}. The state equations for the each partition $n = 1, 2, ..., N$ in the heating coil are shown in (1a) and (1b). The specific heat capacities are c_a and c_w, while $M_{hc,a}$ and $M_{hc,w}$ are the masses of each partition.

$$\dot{T}_{a,n} = \frac{m_a c_a (T_{a,n-1} - T_{a,n}) + G_{hc}(T_{w,n} - T_{a,n})}{M_{hc,a} c_a} \quad (1a)$$

$$\dot{T}_{w,n} = \frac{m_w c_w (T_{w,n-1} - T_{w,n}) + G_{hc}(T_{a,n} - T_{w,n})}{M_{hc,w} c_w} \quad (1b)$$

For $n = 1$, the temperatures $T_{w,0}$ and $T_{a,0}$ equal the intake temperature of the water and air, $T_{w,in}$ and $T_{a,in}$, respectively.

In order to use the model in simulation, it is fitted to experimental data; for multiple settings of air and water flow the logarithmic mean temperature difference is calculated and the total conductance is estimated. Using the least squares method, these data points are then fitted to the polynomial fraction in (2), such that the constants x_1, x_2, and x_3 are determined.

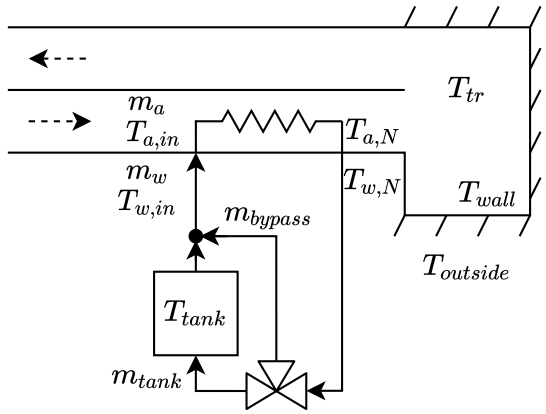

Fig. 4. Overview of the test bed in discharging mode.

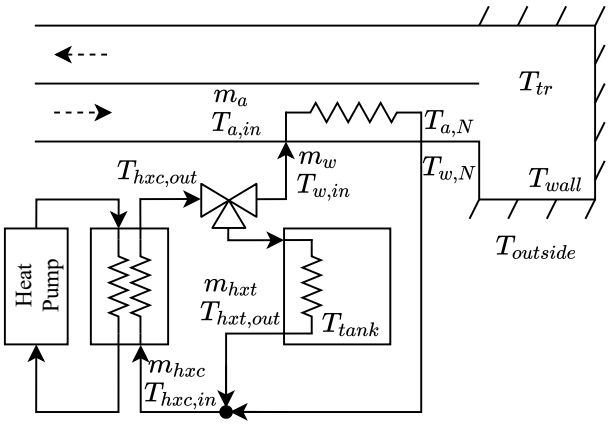

Fig. 5. Overview of the test bed in charging mode.

This allows for the estimation of the total conductance $\hat{G}_{hc,t}$ dependent on the water and air flow.

$$\hat{G}_{hc,t} = \frac{1}{R_c + R_{m_a} + R_{m_w}} \approx \frac{1}{x_1 + x_2 m_a^{-0.8} + x_3 m_w^{-0.8}} \tag{2}$$

In general, conductance G equals the reciprocal of the resistance R. The total thermal resistance of the heating coil in (2) is the sum of the thermal resistances between air and coil R_{m_a}, water and coil R_{m_w}, and of the coil itself R_c [4]. The latter is assumed to be constant. The two other resistances may be expressed by the Nusselt number Nu, which represents the ratio between the convective and conductive heat transfer [4]. Because the conductivity is assumed to be constant, the Nusselt number is proportional to the thermal conductance for each boundary. Hence, R_{m_w} and R_{m_a} are inversely proportional to the Nusselt number of each flow. The Nusselt number can be approximated with Reynold's number Re and Prandtl's number Pr as per the Dittus-Boelter equation shown in (3) [4].

$$Nu \approx 0.023 \cdot Re^{0.8} \cdot Pr^{0.4} \tag{3}$$

The Prandtl number depends only on the characteristics of the fluid and is thus assumed to be constant. Reynolds number however is proportional to the flow of the fluid $(Re \propto m)$ and therefore, the conductance is proportional to the flow to the power of 0.8. Hence, the thermal resistance is proportional to the flow to the power of -0.8 $\left(R \propto m^{-0.8}\right)$.

B. Modeling of the Target Room

The temperature of the air in the target room T_{tr} is dependent on the flow of air in and out, but also the conduction with the wall G_{wall}, as seen in (4).

$$\dot{T}_{tr} = \frac{c_a m_a (T_{a,n} - T_{tr}) + G_{wall}(T_{wall} - T_{tr})}{M_{tr} c_a} \tag{4}$$

The temperature of the walls in the target room T_{wall} depends on the conductance between the air inside the room and the air outside as seen in (5).

$$\dot{T}_{wall} = \frac{G_{wall}(T_{tr} - T_{wall}) + G_{wall,out}(T_{out} - T_{wall})}{M_{wall} c_{wall}} \tag{5}$$

The conductance and mass of the wall are $G_{wall,out}$ and M_{wall} respectively and the specific heat capacity of the wall is c_{wall}. The parameters are estimated using experimental data.

C. Discharging Mode Model

The model diagram for discharging mode is shown in Fig. 4. This model contains the heating coil, water tank, and target room. The water tank has water flow in and out, and it is assumed that no conduction to its surroundings occurs. The corresponding relation is seen in (6). The temperature and mass of the water tank are T_{tank} and M_{tank} respectively.

$$\dot{T}_{tank} = \frac{c_w m_{tank}(T_{w,n} - T_{tank})}{M_{tank} c_w} \tag{6}$$

A mixing equation determines the temperature of the water flowing into the heating coil $T_{w,in}$ as a linear mapping between T_{tank} and $T_{w,N}$, depending on the opening degree OD, as seen in (7).

$$T_{w,in} = T_{tank} \cdot OD + T_{w,N}(1 - OD) \tag{7}$$

D. Charging Mode Model

The model diagram for charging mode is shown in Fig. 5 and contains three heat exchangers: The water tank heat exchanger, the heat pump condenser, and the heating coil. The charging model also includes the model for the target room. The exact dynamics of the condenser and heat pump are disregarded and instead the heat pump is modeled as a system which delivers energy to the water in the condenser heat exchanger. The heat pump behaves like a reversed heat engine, meaning that the heat transferred equals the work done by the heat pump times its Coefficient of Performance (COP) value. For the Carnot cycle the heating COP is $1 + \frac{T_c}{T_h - T_c}$, where T_c and T_h are the temperatures of the cold and hot reservoirs respectively [4]. Since the heat pump is not ideal, the two parts of the COP equation are scaled to account for inefficiencies. Therefore, it is assumed that the change in

energy can be described by the power delivered by the heat pumps compressor P_{comp}, as shown in (8).

$$\dot{Q} \approx x_1 P_{comp} + x_2 \frac{T_c}{T_{hxc,in} - T_c} P_{comp} \tag{8}$$

The temperature of the refrigerant in the evaporator of the heat pump T_c is considered constant. The constants x_1 and x_2 are found by fitting the measured change in energy across the heating coil to (8) using the least squares method.

In the water tank model, it is assumed, that the water in the tank is mixed perfectly, resulting in the tank only having one partition. Thus each of the N partitions in the heat exchanger exchanges heat with the whole tank at once, as seen in (9). The conductance between the water in the heat exchanger and the water in the tank is G_t.

$$\dot{T}_{tank} = \frac{G_t}{M_{tank} c_w} \sum_{n=1}^{N} (T_{hxt,n} - T_{tank}) \tag{9}$$

Each of the N partitions in the heat exchanger are coupled to the previous through the flow of liquid, similar to the heating coil model. The equation for each tank heat exchanger temperature $\dot{T}_{hxt,n}$ is seen in (10).

$$\dot{T}_{hxt,n} = \frac{G_t(T_{tank} - T_{hxt,n}) + m_{hxt} c_w (T_{hxt,n-1} - T_{hxt,n})}{M_{hxt} c_w} \tag{10}$$

For $n = 1$ the temperature $T_{hxt,0}$ equals the input water temperature $T_{w,in}$ which is assumed to equal the temperature after the condenser $T_{hxc,out}$.

IV. Controller Design

A. Discharging Mode Controller

The discharging mode controller has $T_{a,ref}$ as input and an opening degree OD for the valve as output, which indirectly controls $T_{a,N}$. The controller is based on a small signal model around an operating point, which is found in simulation by integral feedback from $T_{a,N}$. The operating point is chosen for m_w, m_a, $T_{a,in}$, and $T_{a,N}$ and are determined by this method for $T_{w,in}$ and $T_{w,N}$. For the controller design, the equations for the heating coil are simplified to $N = 1$ and linearized to the form as seen in (11).

$$\dot{\tilde{x}} = A\tilde{x} + B\tilde{u} = A \begin{bmatrix} \tilde{T}_{a,N} \\ \tilde{T}_{w,N} \end{bmatrix} + B\tilde{T}_{w,in} \tag{11}$$

The matrices A and B are the Jacobians of the state equations in (1) wrt. the states and input respectively. These matrices are used to construct a transfer function as seen in (12).

$$G(s) = \frac{\tilde{T}_{a,N}}{\tilde{T}_{w,in}} = C(sI - A)^{-1}B \tag{12}$$

The matrix C chooses $T_{a,N}$ to be the output, s is the complex frequency, and I is the identity matrix. This second order system is controlled by a PI-controller with a zero placed in the slowest pole of the system and with a gain such that the system attains a phase margin of at least $80°$ ensuring robustness. The temperature $\tilde{T}_{w,in}$ is linearly mapped to an opening degree of the valve. This opening degree is in the simulation limited in rate of change and saturated to represent the physical characteristics of the valve.

B. Charging Mode Controller

In charging mode a similar PI-controller design is employed controlling $T_{a,N}$ via the opening degree of the valve. This controller is also designed by linearizing (1) around a feasible operating point. The main difference between the charging and discharging mode model is the control input being m_w instead of $T_{w,in}$ and different constants, resulting in different A and B matrices. The valve model present in charging mode is approximated using an inverse valve characteristic, transforming opening degree to a flow of water.

To control the charging of the water tank, the output of the heat pump needs to be controlled. A set of P-controllers are designed for this purpose. One P-controller sets the compressor speed based on both the present and targeted valve opening degree. A second P-controller is used to control the water tank temperature, by setting the target valve opening degree for the first P-controller, based on the water tank temperature set-point. To avoid saturation in the PI-controller, the second P-controllers output is limited to the range of 10 % to 90 % opening of the valve. This has the effect, that the water tank is slowly charged even when the water tank temperature set-point is low. The P-controllers are designed using a simulation model and gains are found by direct experimentation.

C. Room Temperature Controller

In both modes, an outer PI-controller uses the error between the room temperature and the room temperature reference to determine the targeted input air temperature. The PI-controller is designed by linearizing (4) and (5) at the reference temperature and determining the transfer function from input air temperature $T_{a,N}$ to room temperature T_{tr}. From the transfer function a Bode plot is used to place the zero and the gain of the PI-controller, to achieve an open-loop response with a phase margin greater than $85°$ to ensure low overshoot.

D. Price Responsive RBC

Based on a moving average algorithm designed by [5], it can be determined, whether the electricity price P is rising, falling or flat, within some upper & lower margins mar_u, mar_l. This is called the price index and takes the values {+1, -1, 0} respectively and is determined by the algorithm shown below. The notation $P_{avg}^{+x,+y}$ is the average electricity price between x and y hours in the forecast.

```
if P < P_avg^{+1,+8} − mar_u or P_avg^{+2,+4} > P_avg^{+2,+10} + mar_u
    price_index = +1
else if P > P_avg^{+1,+8} + mar_l
    price_index = -1
else
    price_index = 0
```

The rules for deciding the operation mode differ for all three price indices. Fig. 6 and 7 show the flowcharts of the RBC for a price index of +1 and -1 respectively. When engaging charging mode, the set-point for the tank temperature

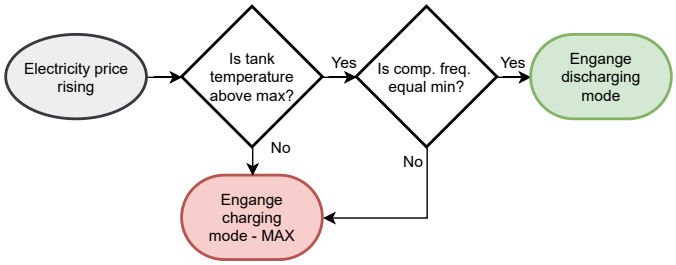

Fig. 6. RBC rules for rising electricity prices (price index = +1).

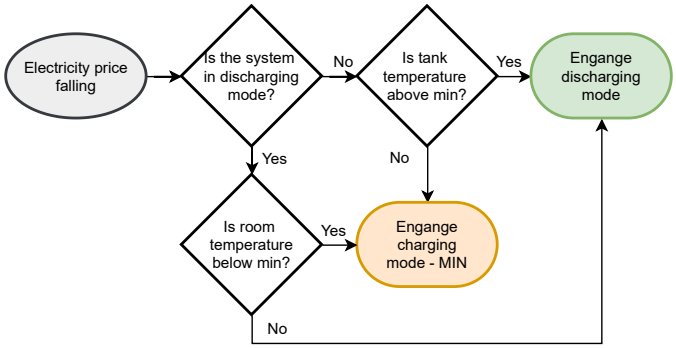

Fig. 7. RBC rules for falling electricity prices (price index = -1).

controller is set to either a maximum (MAX), causing the tank temperature to rise quickly, or minimum (MIN), causing it to rise slowly. These set-points are respectively higher and lower than the tank temperature maximum & minimum, to which the current tank temperature is compared.

For a price index of $+1$ it is favorable to actively charge the tank except for the case of the tank being at max temperature and the heat pump operating at minimum frequency, meaning that the target room is not requesting more heat. In this case the system is forced into discharging mode to avoid wasting energy. For a price index of -1 it is favorable to always discharge the tank unless the room is too cold, or the tank is at the minimum temperature for a sufficient heat supply. The rule set for a price index of 0 differs from that of -1 only by comparing the tank temperature to a normal reference temperature instead of a minimum, allowing for a higher tank temperature before engaging discharging mode.

To determine the effect of the price index algorithm's margins on the RBC price response, the RBC is simulated. To determine the achieved price reduction, the resulting total price is compared to that of a baseline controller. The baseline controller is identical to the rule set for a price index of -1. The system is simulated with the outside temperatures 5, 10, 15 and 20 °C using historic hourly electricity price (HEP) data for two 90 day periods using a variety of different constant margins for the RBC. Period 1 is from 01-01-2021 and Period 2 is from 18-08-2021. The average HEP vary greatly between the two periods, why it is also investigated whether defining the margins dynamically relative to the average HEP four days back yields a greater price reduction.

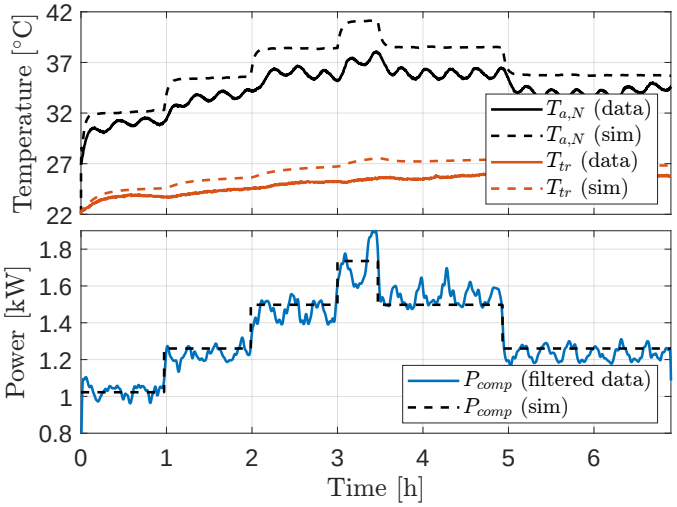

Fig. 8. The ventilation subsystem, target room, and heat pump model responses compared to that of experimental data.

V. Results

A. Model Response

The model equations were implemented in Simulink with the estimated parameters and compared to data from a test with varying compressor frequencies as seen in Fig. 8. It is seen from the figure that $T_{a,N}$ and T_{tr} had some bias in the simulation compared to the test data, but captured the overall behavior except some oscillations introduced by the heat pump.

B. Simulation of Local Controllers

The local controller's response to changes in mode and temperature references, as defined by the RBC, are shown in Fig. 9. It is seen that a change in water tank set-point increased the rate of change of the tank temperature and that the mode decides whether the tank is charged or discharged. Furthermore, the target room temperature was kept close to 24 °C, and when the water tank was discharging the target room temperature did not drop below 1 °C of the reference.

C. Price Responsive RBC

The RBC price reduction, accumulated electricity cost, and the cost per day are shown in Fig. 10. It was found that the RBC can reduce the total electricity cost, compared to the baseline controller. The accumulated costs between baseline and RBC diverged, meaning that the RBC consistently reduces electricity cost. The daily cost in Fig. 10 shows that the RBC behaved similar to the baseline, while reducing cost. The relative cost reduction for the best constant margins for each tested temperature of the first period and the same margins for the second are shown in Table I. This was repeated for relative margins and shown in Table I. It is seen that in the best case the RBC was able to reduce the cost by 6.6 %. If the margin was not relatively defined, the cost for the second period was largely increased. Using the relative margin, the RBC was able to consistently reduce the cost even in the second period.

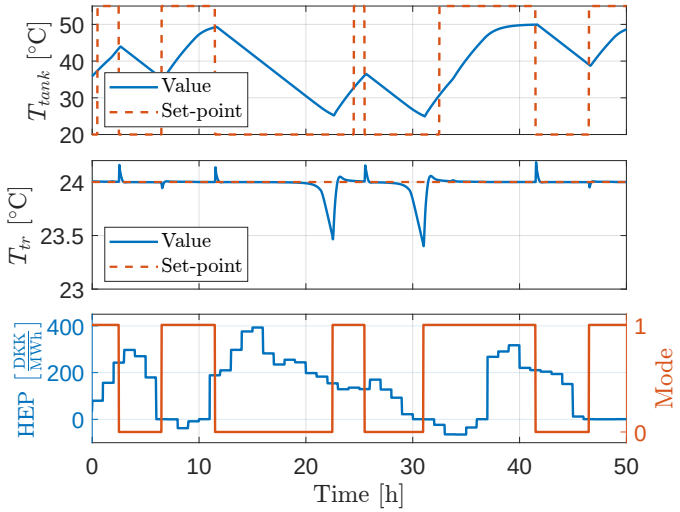

Fig. 9. Water tank temperature and Target room temperature response to changes in mode and water tank temperature set point.

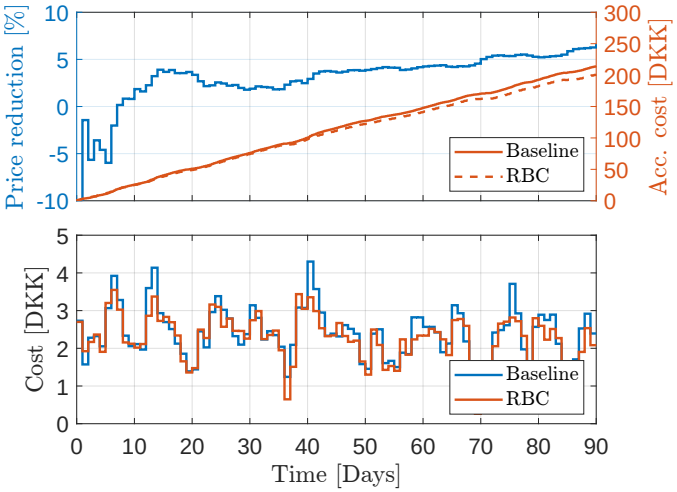

Fig. 10. Price reduction and electricity cost of the RBC compared to a baseline controller, simulated in Period 1, with an outside temperature of 20 °C using best found relative margins.

However, it is also seen that the best margins changed with the temperature, meaning that taking the weather into account could be beneficial. The RBC had the best performance at a higher outdoor temperature. This is likely because the heat pump can generate more excess power and the TES can hold the temperature for longer periods as compared to colder temperatures. This indicates that different dimensions of the physical system could yield better results when it is colder outside.

TABLE I
RBC SIMULATION RESULTS FOR BOTH CONSTANT AND RELATIVE MARGINS. FOR EACH OUTSIDE TEMPERATURE THE BEST FOUND MARGINS ARE SHOWN, AS WELL AS THE REDUCTION IN COST (POSITIVE VALUES EQUAL LOWER COST THAN BASELINE) OVER PERIOD 1 & 2.

Constant Margins				
T_{out} [°C]	mar_u [DKK/MWh]	mar_l [DKK/MWh]	Period 1	Period 2
5	190	40	1.1%	-2.2%
10	140	30	2.5%	-5.5%
15	190	0	2.0%	-11.0%
20	190	0	6.5%	-46.5%
Relative Margins				
T_{out} [°C]	$mar_u[\cdot]$	$mar_l[\cdot]$	Period 1	Period 2
5	0.50	0.20	1.3%	1.3%
10	0.35	0.10	2.3%	1.1%
15	0.50	0.00	2.3%	0.9%
20	0.80	0.05	6.5%	6.6%

VI. Conclusion

It is concluded that it is possible to design and simulate an RBC capable of reducing the total electricity cost of operating the AAU HVAC test bed. This is achieved by shifting loads based on a forecast electricity price. The test bed is divided into two operation modes, charging and discharging. In discharging mode, the system heats the target room with energy that is stored in the TES while the system is in charging mode. The system is modeled using state space equations and fitted to experimental data. A cascading PI controller is designed, for which the inner control loop depends on the operation mode. It is shown via simulation, that the target room temperature does not deviate more than 1 °C from its reference at any time. A price responsive RBC is designed, based on a price indexing algorithm, indicating whether the forecast electricity price is rising or falling. The RBC decides which operation mode the system should be in and how much energy should be stored in the TES. By tweaking the price indexing algorithm, it is found, that the RBC can reduce the total electricity cost by 0.9 % to 6.6 %, dependent on the outside temperature.

VII. Acknowledgements

The authors would like to thank Roozbeh Izadi-Zamanbadi and Tommy Friis Jensen from Danfoss for aiding in the setup of the HVAC testbed and setup of the heat pump subsystem in particular. Furthermore the authors thank Pierre Vogler-Finck and Alex Arash Sand Kalaee from Neogrid for providing their technology and support.

References

[1] K. Li, J. Cursio and Y. Sun, "Principal Component Analysis of Price Fluctuation in the Smart Grid Electricity Market," *Basel*, vol. 10, iss. 11, pp. 4019-4035, November 2018.

[2] K. Lee, M. Joo, and N. Baek, "Experimental Evaluation of Simple Thermal Storage Control Strategies in Low-Energy Solar Houses to Reduce Electricity Consumption during Grid On-Peak Periods," *Energies*, vol. 8, no. 9, pp. 9344-9364, August 2015.

[3] L. Schibuola, M. Scarpa and C. Tambani, "Demand response management by means of heat pumps controlled via real time pricing," *Energy and Buildings*, vol. 90, pp. 15-28, March 2015.

[4] G. Hundy, A. Trott and T. Welch, "Chapter 1 - Fundamentals" in *Refrigeration, Air Conditioning and Heat Pumps*, Fifth Edition, Cambridge UK: Butterworth-Heinemann, 2016, pp. 1-18, ISBN 9780081006474.

[5] B. Alimohammadisagvand, J. Jokisalo, K. Sirén, "Comparison of four rule-based demand response control algorithms in an electrically and heat pump-heated residential building", *Applied Energy*, vol. 209, pp. 167-179, January 2018.